Generalized Synchronous Optimal Pulse Width Modulation for Multilevel Inverters

Jackson Lago and Marcelo Lobo Heldwein, *Senior Member, IEEE*

***Abstract*—With the growing interest of the industry in high-power medium-voltage multilevel inverters and the technological limitation in high voltage power semiconductors switches, synchronous optimal pulse width modulation techniques, originally developed for two-/three-level inverters, became again a topic of interest, now to optimize multilevel waveforms. This work proposes a novel formulation for the problem of optimizing the modulation pattern of multilevel converters, including in a single optimization problem the decision of the directions for each step transition in addition to the switching angles and, thus, completely defining the optimized multilevel waveform at a given modulation index. In addition, experimental results are presented in order to demonstrate the effectiveness of this optimized modulation technique exemplar applied to a five-level NPC H–bridge feeding a permanent magnet synchronous motor.**

***Index Terms*—Inverters, multilevel systems, pulse width modulation.**

I. Introduction

THE ground concept for synchronous modulation schemes based on a set of predefined (offline evaluated) optimized switching angles emerged in the 1960s in order to make good use of the low switching frequency allowed for the semiconductor technology at that time. Initially, the technique was used to completely eliminate a group of harmonics components in two-level inverters, known as Selective Harmonic Elimination (SHE) [1]. Soon later, Buja and Indri [2] proposed to do not completely eliminate a limited group of harmonic components, but instead to control a whole spectrum to minimize the harmonic distortion of the current in a motor. This assumed the motor mathematical model and waveform performance indexes such as Total Harmonic Distortion (THD) and Weighted THD (WTHD). This technique, also developed to two- and three-level inverters, became known as Synchronous Optimal Pulsewidth modulation (SOP), sometimes also referred as Optimized Pulse Pattern. In the following decades, with the evolution of faster power semiconductors enabling higher switching frequencies, the interest on SOP was virtually lost in low-voltage/-power applications. Recently, with the advent of multilevel converters for powering very high power medium voltage systems, which are also subject to restrictions of low switching frequency, this technique became again a topic of research interest [3]–[14].

The mathematical formulation for the optimization of two-level inverters waveforms (and also three-level waveforms with the restriction of use only positive levels within the positive semicycle) is well establish and extensively studied [15]–[21]. The output waveforms can assume only two levels within a semicycle, and consequently, consecutive switchings just toggle the level of the output waveform such that the direction of each step transition is imposed and well defined in the two- and three-level cases. Thus, a two-level waveform is fully defined by a set of switching angles $\boldsymbol{\alpha} = \{\alpha_1, \alpha_2, \ldots, \alpha_N\}$ that holds only the information about the transition angles. However, for multilevel inverters with number of levels L larger than three, each transition from intermediary levels can assume two directions. This results in additional degrees of freedom. Thus, for the modulation of a multilevel inverter it is not enough to define the switching angles of the output waveform. The transition directions are also needed. The original formulation for the two-/three-level waveform optimization problem is such that optimal switching angles $\boldsymbol{\alpha}$ are obtained as the result of an optimization problem that minimizes a given performance index computed from the harmonic spectrum of the resulting waveform. This formulation does not include the decision of the transition direction and, thus, it cannot be directly used for optimizing multilevel waveforms.

Since SOP techniques are based on the optimization of voltage harmonic spectra it is reasonable to assume that the degree of freedom related to the transition directions appears in the computation of the Fourier coefficients of the resulting waveform. An expression that defines the amplitude of each harmonic components of the multilevel waveform as a function of the instants of each commutation and their directions is desirable. A generic L-level waveform (for odd values of L) with N commutations within $0 \leq \theta < \pi/2$ and quarter-wave symmetry can be decomposed by N unity step functions $u(x)$, each one phase shifted by α_k and multiplied by an unitary coefficient $\delta_k \in \{-1, +1\}$ that defines the direction of the step at instant α_k, where $k = 1, 2, \ldots, N$. Thus

$$l(\theta) = \sum_{k=1}^{N} \xi_k(\theta) = \sum_{k=1}^{N} \delta_k u(\theta - \alpha_k), \quad 0 \leq \theta < \pi/2 \quad (1)$$

Manuscript received January 16, 2016; revised May 24, 2016 and September 17, 2016; accepted October 19, 2016. Date of publication October 25, 2016; date of current version March 24, 2017. Recommended for publication by Associate Editor Xinbo Ruan.

J. Lago is with the Power Electronics and Industrial Drives Research Group, Federal Institute of Education, Science and Technology of Santa Catarina, Florianopolis 88020-300, Brazil (e-mail: jacksonl@inep.ufsc.br).

L. Heldwein is with the Department of Electrical Engineering, Federal University of Santa Catarina, Florianopolis 88040-970, Brazil (e-mail: heldwein@inep.ufsc.br).

Color versions of one or more of the figures in this paper are available online at http://ieeexplore.ieee.org.

Digital Object Identifier 10.1109/TPEL.2016.2621022

See http://www.ieee.org/publications_standards/publications/rights/index.html for more information.

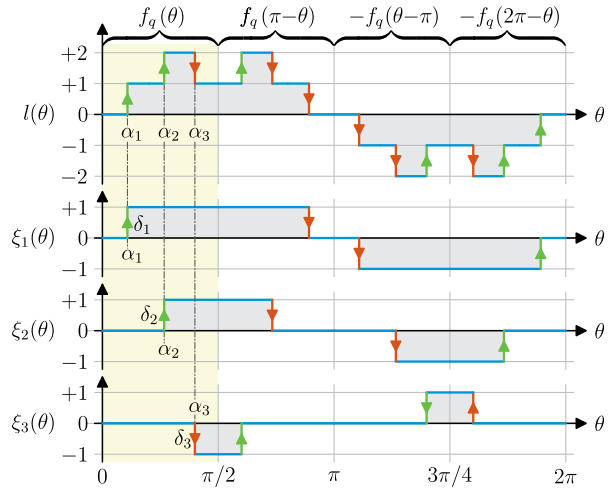

Fig. 1. Waveform decomposition in N elementary three-level signals.

where $l(\theta)$ is the instantaneous voltage level of the output waveform and $u(x)$ is the unity step function defined as

$$u(x) = \begin{cases} 0 & \text{if } x < 0 \\ 1 & \text{if } x \geq 0 \end{cases}. \tag{2}$$

Fig. 1 illustrates this decomposition and the symmetry relations that define the signals in a period, where $f_q(x)$ stands for the function that defines the signal in the first quarter of the period. It is important to notice that the signals ξ_k are simply a mathematical decomposition of the voltage output waveform and are not independently physically synthesized by different components of the power electronics structure of the inverter.

The harmonic contents of the elementary signals $\xi_k(\theta)$ that composes the multilevel waveform are defined by

$$\hat{\xi}_{k,h}\left(\alpha_k, \delta\right) = \frac{4}{\pi h}\delta\cos(h\alpha_k) \tag{3}$$

where $\hat{\xi}_{k,h}$ is the amplitude of the h-order harmonic component of the signal $\xi_k(\theta)$.

From (1) and (3) it is possible to find an expression that defines the harmonic contents of a generic multilevel waveform with quarter-wave symmetry as a function of the switching angles $\boldsymbol{\alpha}$ and transition directions $\boldsymbol{\delta}$ as

$$\hat{l}_h\left(\boldsymbol{\alpha}, \boldsymbol{\delta}\right) = \frac{4}{\pi h}\sum_{k=1}^{N}\delta_k\cos(h\alpha_k) \tag{4}$$

where $\hat{l}_h$ is the amplitude of the harmonic component of order h of the inverter output waveform, N is the number of switchings in a quarter of the waveform, and α_k and δ_k are, respectively, the k-th elements of the set of switching angles $\boldsymbol{\alpha}$, and the set of the signs that represent the direction of each step transition $\boldsymbol{\delta}$ that define the waveform

$$\begin{aligned} \boldsymbol{\alpha} &= \{\alpha_1, \alpha_2, \ldots, \alpha_N\}, \quad 0 < \alpha_1 < \alpha_2 < \cdots < \alpha_N < \pi/2 \\ \boldsymbol{\delta} &= \{\delta_1, \delta_2, \ldots, \delta_N\}, \quad \delta_k \in \{-1, +1\}. \end{aligned} \tag{5}$$

With (4) it is possible to evaluate the WTHD (6), or similar performance indices, of the inverter output voltage waveform

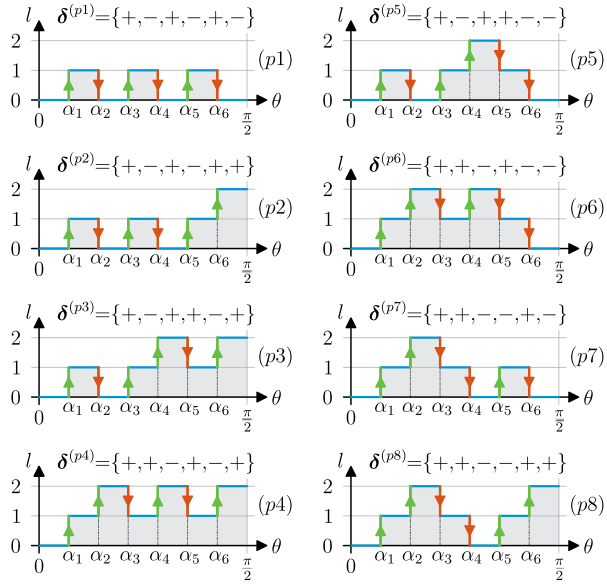

Fig. 2. Eigth possible switching patterns for a waveform with $L = 5$ and $N = 6$ and quarter-wave symmetry.

and use it as the objective function for the optimization problem. However, a minimization problem that must return the two sets, angles set, and directions set, is a mixed integer nonlinear problem. There is no efficient optimization algorithm for this type of problem and nor it is possible to ensure a solution for this kind of formulation

$$\sigma_{\text{wthd}}\left(\boldsymbol{\alpha}, \boldsymbol{\delta}\right) = \sum_{\substack{h=6n\mp1 \\ n\in\mathbb{N}^*}}^{H}\left[\frac{4}{\pi h^2}\sum_{k=1}^{N}\delta_k\cos(h\alpha_k)\right]^2. \tag{6}$$

To overcome this complexity Rathore *et al.* [22] introduced the concept of switching structures, also known as switching patterns. A switching pattern is a valid sequence of the direction of the step transitions along the waveform. Each switching pattern completely defines the $\boldsymbol{\delta}$ set in (4) and (6). For instance, a five-level inverter ($L = 5$) with six switching angles in a quarter of the output waveform ($N = 6$) has eight different valid switching patterns as seen in Fig. 2.

Solving the optimization problem for a single switching pattern, imposing $\boldsymbol{\delta}$, is mathematically similar to solving the problem of a two-/three-level waveform. Since the switching angles $\boldsymbol{\alpha}$ for a given modulation index M can be obtained by solving the optimization problem for a defined switching pattern. The remaining problem is to define the ideal switching pattern for each modulation index M value, defined by

$$M = \frac{2\hat{V}_1}{(L-1)E}, \quad M \in \left(0, \frac{4}{\pi}\right) \tag{7}$$

where $\hat{V}_1$ is the amplitude of the fundamental output phase voltage, E is the voltage of each voltage level, and L is the number of phase voltage levels allowed by the converter power structure.

Some authors [23]–[26] define a pattern and optimize the switching angles assuming the chosen pattern gives acceptable results. In fact, the optimal pattern is dependent of the mod-

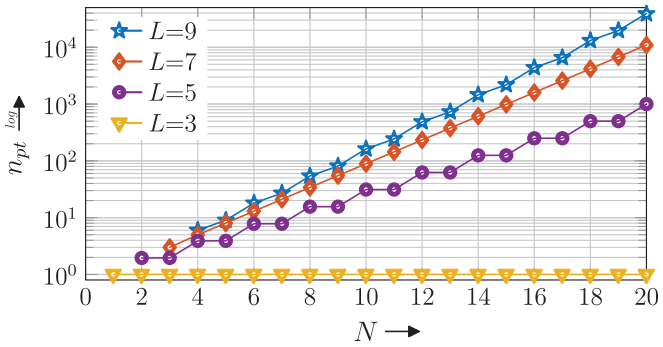

Fig. 3. Number of possible switching patterns for a L–level multilevel converter with N commutations in a quarter of the fundamental period.

ulation index M that is part of one of the constraints of the optimization problem and an optimal solution for the modulator will change the pattern for different ranges of M. In order to get an optimum set of switching angles and the optimal pattern for each modulation index value, Rathore *et al.* [22] propose to evaluate the optimization problem for the entire range of interest of the modulation index M for each valid switching pattern and then select the pattern and its corresponding switching angles that give the optimum solution. This technique allows to find the optimal solution, both, for the switching angles and the switching patterns completely defining $\boldsymbol{\alpha}$ and $\boldsymbol{\delta}$. However, the number of switching patterns and consequently the scale of the optimization problem that must be solved can be impractically large for operation with a relatively high number of commutations per cycle or for an inverter with a high number of levels. The increase of the number of different valid patterns for inverters with three-, five-, seven- and nine-level waveforms for up to 20 commutations in a quarter of the fundamental period is shown in Fig. 3. The number of valid switching patterns graphically shown in Fig. 3 can be computed by (8), where $\boldsymbol{A}$ is the adjacent matrix of the graph that represents the change of level possibilities in the first quarter of the waveform using only adjacent states. Thus

$$n_{\text{pt}} = \sum_{j=1}^{2-\text{mod}(L,2)} \sum_{i=1}^{\left\lfloor \frac{L+1}{2} \right\rfloor} [\boldsymbol{A}]_{j,i}\,. \tag{8}$$

Other attempts to adapt the two-level optimized modulation to multilevel ones were [22], [25]–[31]. Most of them use the concept of switching patterns and/or impose unnecessary restrictions in order to simplify the optimization problem. Analytical solutions of the optimization problem and selective elimination are explored in [23], [24], [32], however, to achieve these analytical solutions various constraints are imposed on the problem, and even the selection of the objective function is limited to minimize the THD of voltage rather than the current. This work extends [14] approach and proposes a generalized formulation of the optimization problem for multilevel waveforms that does not use the concept of switching patterns and includes the transition direction decision within thew optimization problem as an expansion of the search space of the optimization variables.

II. SOP Modulation Generalization for Multilevel Converters

Since the direction of the steps of multilevel waveforms are modeled as a set of binary variables ($\boldsymbol{\delta}$), it turns the optimization problem into a mixed integer nonlinear one. The adaptation for the optimization problem formulation presented in this section reduces this problem to a nonlinear problem without imposing any simplification nor losing generality. The intrinsic symmetries of the problem are the basis for this.

An optimization algorithm to minimize (6), or a similar index as a function of the Fourier coefficients, must return the optimized values for both $\boldsymbol{\alpha}$ and $\boldsymbol{\delta}$ that represent, respectively, the set of angles (relative to the fundamental period) where the step transitions occur and the transition directions.

A generalized expression to evaluate the amplitude of any harmonic component of a multilevel waveform was presented in (4). This expression is the central point for the optimization problems based on harmonic components control and is the one that holds the relationship between the two sets of variables to be found. The cosine term in (4) is a direct consequence of the choice of having the fundamental component of the output waveform in phase with a sine signal with the same frequency. Shifting the entire waveform by $\pi/2$ rad, the fundamental component of the waveform becomes in phase with a cosine signal, and the expression for the harmonic content of the waveform is now given by

$$\hat{l}_h\left(\boldsymbol{\alpha},\boldsymbol{\delta}\right) = \frac{4}{\pi h}\sum_{k=1}^{N}\delta_k \sin(h\alpha_k). \tag{9}$$

This reference shift adopted in the formulation turns the cosine term in (4) into a sine term in (9) and the odd symmetry of the function sine can be used to join the two set of variables $\boldsymbol{\alpha}$ and $\boldsymbol{\delta}$ as a new set of variable $\boldsymbol{\gamma}$ with

$$\begin{aligned}\hat{l}_h\left(\boldsymbol{\alpha},\boldsymbol{\delta}\right) &= \frac{4}{\pi h}\sum_{k=1}^{N}\sin(h\delta_k\alpha_k)\\ &= \hat{l}_h\left(\boldsymbol{\gamma}\right) = \frac{4}{\pi h}\sum_{k=1}^{N}\sin(h\gamma_k)\end{aligned} \tag{10}$$

where

$$\gamma_k = \delta_k\alpha_k, \qquad -\pi/2 < \gamma_k < \pi/2 \tag{11}$$

and since α_k is always positive and δ_k has only a sign information with fixed amplitude, both α_k and δ_k can be completely reconstituted from γ_k using

$$\begin{aligned}\alpha_k &= \text{abs}(\gamma_k), \quad 0 < \alpha_k < \pi/2\\ \delta_k &= \text{sign}(\gamma_k), \quad \delta_k \in \{-1,+1\}\end{aligned} \tag{12}$$

without losing information. This ensures that this procedure does not affect the validity or generality of the optimization problem formulation.

Expression (10) is valid only for odd level waveforms. Inverters with even levels have lesser practical interest, but a similar expression can be derived just adding a term $\frac{1}{2}\xi_0(0)$ that models

the commutation from $l=-1$ to $l=+1$ at $\theta=0$ for even level waveforms. Thus

$$\hat{l}(\boldsymbol{\gamma})=\begin{cases}\dfrac{4}{\pi h}\sum_{k=1}^{N}\sin(h\gamma_k) & \text{if } L \text{ is odd}\\ \dfrac{4}{\pi h}\sum_{k=1}^{N}\sin(h\gamma_k)+\dfrac{2(-1)^{\frac{h+1}{2}}}{\pi h} & \text{if } L \text{ is even}\end{cases}. \tag{13}$$

The complete WTHD minimization problem of a generic odd level waveform is then

$$\min_{\boldsymbol{\gamma}} \sum_{\substack{h=6n\mp1\\ n\in\mathbb{N}^*}}^{H}\frac{16}{\pi^2h^4}\left[\sum_{k=1}^{N}\sin(h\gamma_k)\right]^2$$

$$\text{subject to}\begin{cases}-\pi/2\le\gamma_k\le\pi/2\\ \dfrac{4}{\pi}\sum_{k=1}^{N}\sin(\gamma_k)=M\\ 0\le l(\gamma_k^+)\le(L-1)/2\\ \boldsymbol{A\gamma}\le\boldsymbol{\Delta\gamma}_{\min}\end{cases} \tag{14}$$

where H is the highest considered harmonic order, h is the harmonic order, L is the maximum number of levels that the inverter can synthesize, N is the number of switchings performed in a quarter-wave, and $l(\gamma_k^+)$ is the level of the waveform after the transition at angle α_k. The first constraint of (14) ensures the validity of the range of the found angles, the second one sets the amplitude of the fundamental component to achieve the desired modulation index M, and the third ensures that the solution does not use more levels than the inverter can synthesize. In fact, the third constraint can be relaxed if $M<1$. The fourth constraint is the set of linear inequalities given by

$$\begin{pmatrix}1&-1&0&\cdots&0\\0&1&-1&\cdots&0\\\vdots&\vdots&\vdots&\ddots&\vdots\\0&0&0&\cdots&-1\\0&0&0&\cdots&1\end{pmatrix}\begin{pmatrix}\gamma_1\\\gamma_2\\\vdots\\\gamma_{N-1}\\\gamma_N\end{pmatrix}\le\begin{pmatrix}-\Delta\gamma\\-\Delta\gamma\\\vdots\\-\Delta\gamma\\\frac{\pi}{2}-\Delta\gamma\end{pmatrix} \tag{15}$$

that ensure a minimum pulse width $\Delta\gamma$, avoiding double level commutations. This linear inequalities also sort the elements of $\boldsymbol{\gamma}$, which is important since all elements permutations in $\boldsymbol{\gamma}$ are valid representations of a same waveform. This results in at least $N!$ multiple global minimums that significantly increases the complexity of the optimization problem.

The proposed algorithm does not impose the number of level of the optimal waveform. It just limits the maximum number of levels that can be used. The actual number of levels of the optimal waveform is result of the optimization problem as a consequence of the found optimal angles and switching directions and can assume any odd number lower than the maximum number of levels imposed by constraints on the optimization problem.

To validate this unified formulation of the optimization problem for a multilevel waveform, the solution found with this formulation can be compared against the results found with the technique that optimizes the switching angles individually for all possible switching patterns. The proposed algorithm is not expected to give better results than existing algorithms, but the same optimal results obtained directly from a true multilevel waveform optimization that includes in a single optimization problem the direction of each switchings, in addition to the optimal angles. Fig. 4 shows the values of the objective function obtained by numerically solving (14) and its equivalent formulations with the conventional method [22] for the four possible switching patterns of a waveform with $N=5$ and $L=5$. The nonlinear numeric solvers pack KNITRO was used to solve the optimization problems in both formulations. This comparison shows that the proposed formulation is able to find the optimal solution minimizing, in this case the WTHD of the waveform, for the entire valid modulation index range, obtaining both the optimal angles and the optimal switching pattern through the set of variables $\boldsymbol{\gamma}$ as a solution of an unified optimization problem.

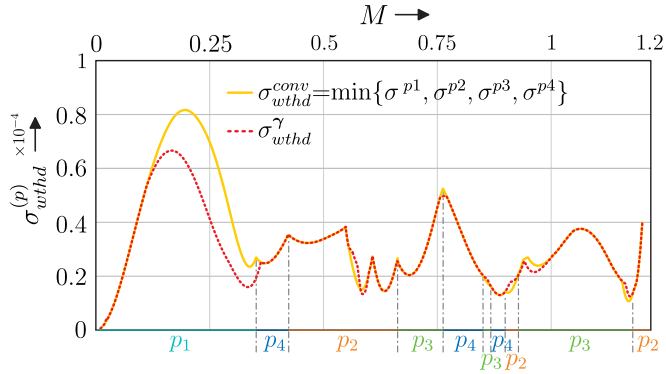

Fig. 4. Comparison between the minimum value for the objective function found by the proposed formulation ($\sigma^{\gamma}_{\text{wthd}}$) against the conventional method ($\sigma^{\text{conv}}_{\text{wthd}}$ is the minimum of all possible switching patterns $p_1 \ldots p_{n\,\text{pt}}$), emphasize the optimal switching pattern for each modulation index range.

Even though the new formulation is slightly more complex, it is more flexible and leads to smaller optimization times, which might be particularly important for a large number of levels/switching times or for more complex metrics.

It is known that optimizing a multilevel waveform for indexes like THD and WTHD often result in a set of optimum switching angles with many discontinuities with respect to the M axis. In order to reduce the occurrence of such discontinuities, Rathore *et al.* [3] perform a post optimization that takes advantage of a deficiency of nonlinear optimization algorithms that cannot guarantee that the result is the global minimum, which often is only a local minimal in the vicinity of the starting point supplied to the algorithm. In this case, the last optimum angles set and pulse pattern is adopted as starting point passed to the numeric solver and the optimization problem is recalculated. In the present work such discontinuities are not forbidden but penalized instead. Fig. 5 shows the algorithm used to perform such discontinuities penalization. Since it is a nonlinear problem, there are no means to ensure that the result of the optimization is a global minimum, so three different starting points are provided to the numerical solver (multistart) to increase the likelihood of finding a global minimum. The first one is the optimal angles set previously obtained for a slightly lower M as the approach in [3]. The other starting points are the

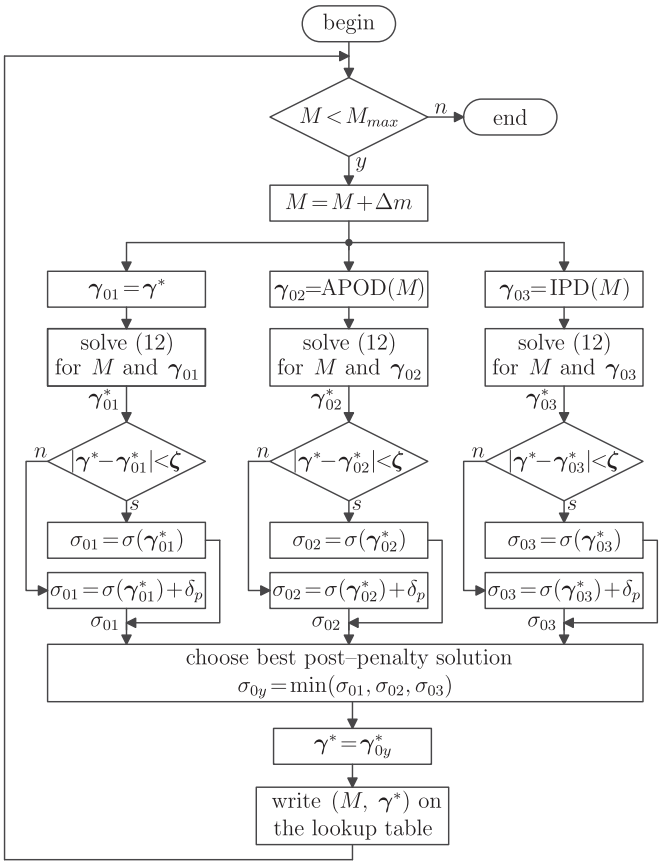

Fig. 5. Optimal solutions discontinuities penalty algorithm.

equivalent switching angles generated by the carrier-based multilevel modulation techniques In Phase Disposition (IPD) and Alternate Phase Opposite Disposition. Even though three starting points have been used in the results obtained in this work, more starting points could be used to further increase the probability of finding global minima. The choice of three starting points was made empirically since tests with more starting points did not show relevant improvements in the solutions for the metric and scale of the optimized problems. The optimal angles that result from these three starting points are tested for discontinuities and a penalty is applied to the value of the objective functions for the discontinuous ones. The post penalty results are compared and the best result is chosen. This allows us to control through the penalty factor δ_p how much better is the harmonic distortion obtained with a discontinuous result so that it is not discarded.

The majority of multilevel inverters are used within electric motor drives and the inverter must be able to control its output voltage amplitude and frequency in a wide range to drive the motor with angular speed from zero up to rated value. In the SOP schemes, unlike conventional carrier-based ones, the switching frequency is dependent on the output fundamental frequency, which means that during speed variations the switching frequency is constantly changing. Thus, for low fundamental output frequency the number of commutations per cycle N can be increased to reduce distortion without over stressing the

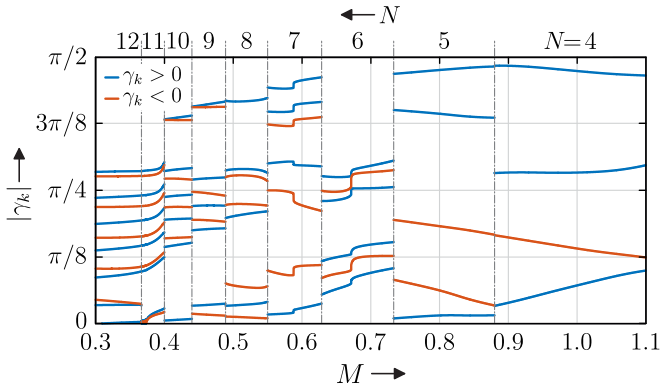

Fig. 6. Optimal values of $\boldsymbol{\gamma}$ from $N = 12$ down to $N = 4$ for a five-level inverter with constant V/f and maximum device switching frequency limited at $f_{sw} = 188$ Hz.

semiconductor switches due to switching losses. Since a motor operates with a nearly constant voltage per frequency (V/f) relation, the switching frequency is proportional to M, and a table with the values of the optimal $\boldsymbol{\gamma}$ with variable discrete values for N can be generated to provide the optimal modulation with maximum frequency limitation for all the range of voltage/fundamental frequency operation.

Fig. 6 shows the optimal $\boldsymbol{\gamma}$ for modulation indexes $0.3 \leq M \leq 1.1$ with varying the number of commutations per cycle from $N = 12$ down to $N = 4$. For very low output frequencies, this technique of variable N is not appropriate since N should be changed too often for small changes of M and frequency. This could result in several N changes within the period of the fundamental depending on the increasing ratio of the output frequency during the acceleration of the motor. A different modulation technique such as a carrier-based one can be used during the initial stage of the motor acceleration to solve that for very low fundamental frequency. The modulation technique can be switched to the SOP when the fundamental frequency becomes greater than a predefined minimum value.

The modulation implementation is split into two steps, in a similar way to what is done in Space Vector Modulation (SVM). The first step is offline computed and determines the optimal output voltage waveform for the entire M range (switching table from Fig. 6) without worrying about how these waveforms can be synthesized by the inverter and neither with its eventually required internal energy balance. The second step is responsible for, in real time, generating the gate signals for the controlled switches that synthesize the given predefined waveforms and simultaneously provide further inverter features, such as the internal voltage balances by choosing the appropriate redundant states. This can be performed in all power structures that have enough redundant states to balance the dc-bus voltages without distorting the output waveforms, including the NPC H-bridge.

III. Experimental Results

A low-voltage 15 kW prototype of a five-level NPC H-bridge inverter (HNPC) was built. The complete experimental setup is seen in Fig. 7. It comprises the three-phase HNPC inverter fed by three 12-pulse rectifiers and a 11 kW permanent magnet

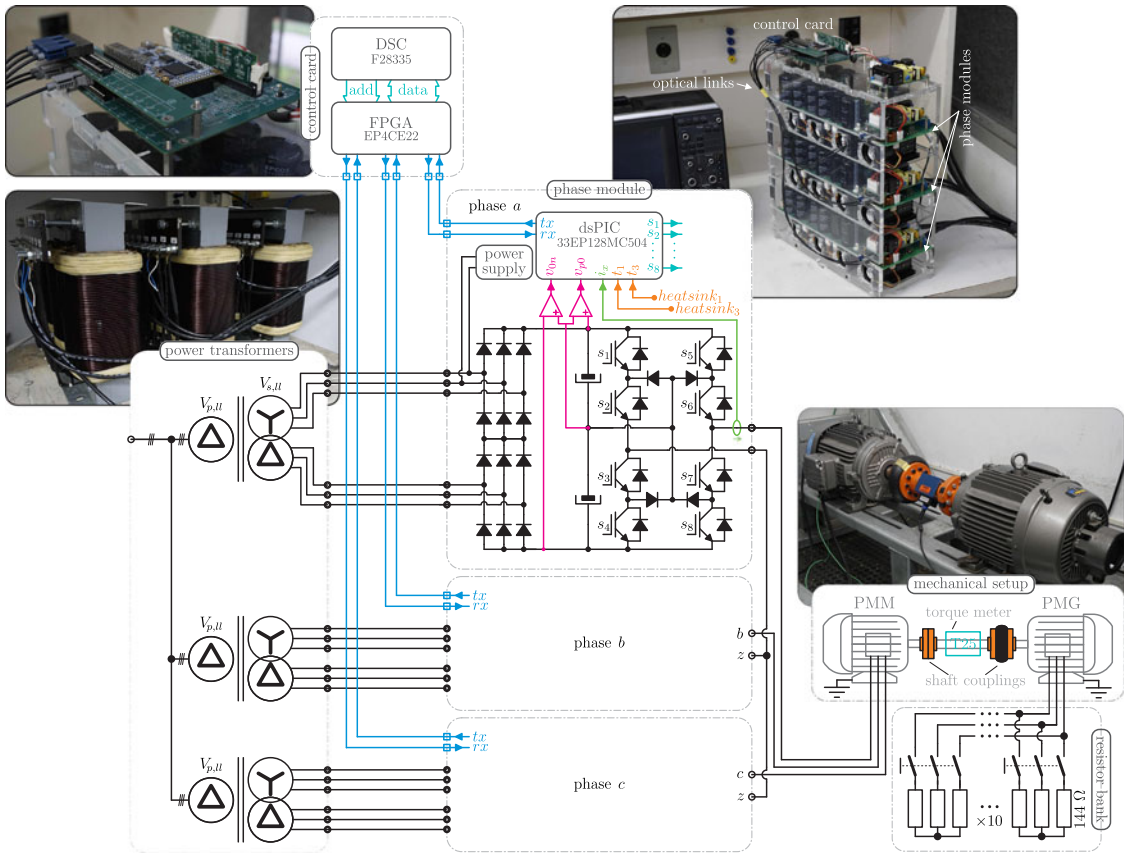

Fig. 7. Experimental setup showing the five-level converter, its control board and rectifier transformer, as well as the PMSM machine lab bench and load scheme.

TABLE I
EXPERIMENTAL SETUP SPECIFICATIONS

12-Pulse Rectifier			
f_g	60	Hz	Mains frequency
$V_{p,\text{ll}}$	380	V	Rated primary rms voltage
$V_{s,l}$	120	V	Rated secondaries rms voltage
$V_{\text{pn, avg}}$	290 to 320	V	dc links average voltage range
HNPC Inverter			
L	5	–	# of levels of phase voltage
M	0 to 1.1	–	Modulation index range
f_1	0 to 90	Hz	Fundamental frequency range
f_{sw}	90 to 2160	Hz	avg device switching frequency
C_{pn}	2	mF	Equivalent link capacitance
PMSM			
P_r	11	kW	Rated shaft power
$V_{r,\text{ll}}$	380	V	Rated line–to–line rms voltage
I_r	19.2	A	Rated rms current
f_r	90	Hz	Rated frequency
p	3	–	# of pole pairs
w_r	1800	rpm	Rated angular velocity
T_r	58.4	Nm	Rated torque

synchronous motor (PMSM) as load. The motor is mechanically connected to a permanent magnet synchronous generator that feeds a resistive load in order to generate the PMSM torque. The system specifications are in Table I.

The SOP modulation scheme is a synchronous modulation based on a lookup table (like Fig. 6) with the optimum commutation angles and directions obtained from solving the previously presented optimization problem (14). The real time reconstruction of the phase voltages from a table of γ and the generation of the gate signals for the eight power electronic switches of each phase of the inverter is performed in the control card.

The individual HNPC modules dc-link central point voltage balance is achieved by choosing the appropriate intraphase redundant states that tends to restore the balance based voltage and current measurements in real time at each module. To act on the balance only by choosing redundant states ensures that the power stage of the inverter imposes to the load the optimal output voltage waveform computed offline. The use of redundant states does not lead to simultaneous switching of two or more levels since only adjacent states are used. Fig. 8 shows the state machine with which the states are chosen and how each state affects the voltage balance. In the case of a five-level HNPC only the states with levels $+1$ or -1 affect the dc-link balance of each phase since for levels $+2$, -2, and 0 the dc-link capacitors are not inserted in the path of the output current. For example: a switching transition occurs that reduces the voltage level of one of the phases from $l = +2$ (state 1) to $l = +1$ (states 2 or 3). Both states (2 and 3) are adjacent to state 1. Choosing accordingly the state 2 or 3 depending on the voltage unbalance will act in opposition to the imbalance and since both (states 2 and 3) are adjacent to 1, no additional switching transitions or level steps are needed.

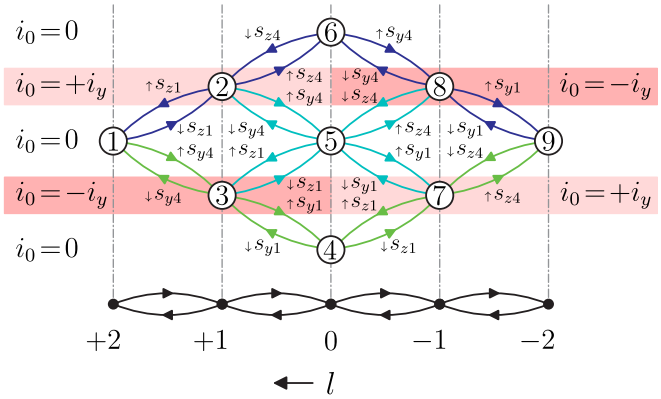

Fig. 8. Diagram of the possible states of a phase, the adjacency between them, and how each state affects the dc-link voltage balance.

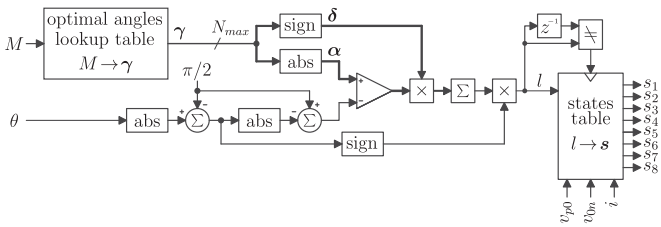

Fig. 9. Output phase voltage signal reconstruction from γ and gate signal generation.

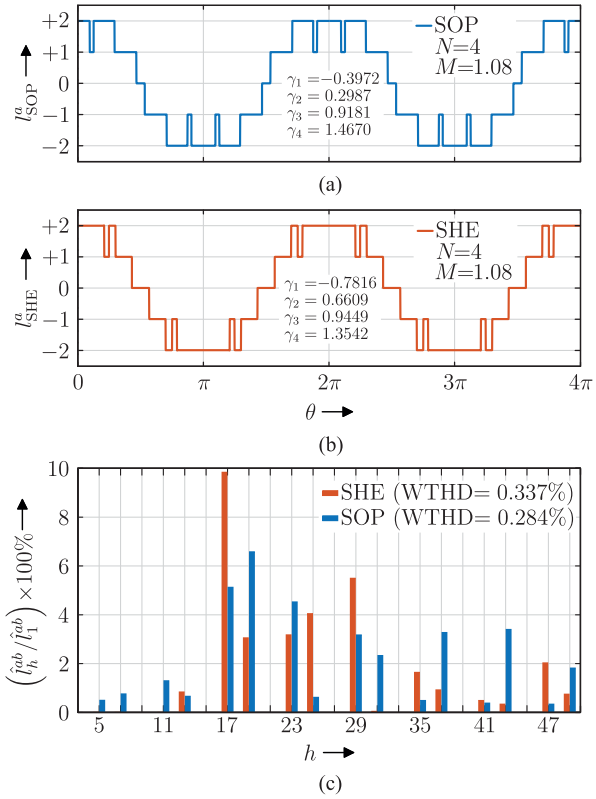

Fig. 10. Voltage output waveform examples for (a) SOP and (b) SHE modulation with $N = 4$ and $M = 1.08$, and (c) the line-to-line voltage harmonic spectrum comparison between them.

The control and modulation algorithms are centralized and run in a central control board based on a Digital Signal Controller and a Field Programmable Gate Array. Each phase module has its own local microcontroller, communicating with the central control board through optic fiber links, similar to the platform used in [33]. The gate signals of all controlled switches are generated by the centralized modulator, in which the algorithm described in Fig. 9 is implemented and signals are transmitted to the local controllers which are responsible for the command of the insulated gate bipolar transistor (IGBT) gate signals besides performing local measurements and protection.

A comparison against three known modulation techniques to evaluate the effectiveness of the proposed SOP modulation for a wide switching frequency range was experimentally performed. The first modulation is a synchronous SHE modulation with cancellation of the $(N-1)$ nontriplen lower order voltage harmonic components [34]–[42]. As the multilevel SHE modulation shares the same problem regarding the determination of each transition direction as the SOP modulation, the γ formulation proposed in this work was also used in the SHE problem formulation. This is done by adding a new set of constraints in order to impose the required harmonic cancellation to the optimization problem (14). This approach also ensures that the SHE switching angles set used, among the multiple valid solution sets for which the SHE requirements are met, is the one that leads to the lower current distortion. This being the multilevel equivalent to what is proposed by Agelidis *et al.* [41] for the two-level case. The second modulation is a five-level seven-segments regularly sampled SVM [43], [44]. The third is named here modified IPD (mIPD) is a carrier-based and consists of an adaptation of the IPD modulation for the HNPC, where the five-level phase voltage reference waveform is generated by two three-level IPD modulators phase shifted by π rad to balance the voltages and losses between the two NPC legs that compose each module of the HNPC [44]. All modulation techniques were implemented in the same prototype and the experiments were carried out in very similar conditions, with the same load, input voltage levels, and M.

Fig. 10(a) and (b) illustrates the waveforms generated by, respectively, the SOP and the SHE modulators, both for $N = 4$ and $M = 1.08$. Fig. 10(c) shows the differences in the harmonic spectrum of the line-to-line voltage for the two used modulations in the case at hand. As expected, the SHE modulation completely cancels the lower order harmonic components (in this case $h = 5, 7, 11$) at the expense of higher amplitudes of some noncontrolled harmonic components (particularly $h = 17$ in this case). The SOP modulation does not cancel any harmonic component but instead controls the amplitude of the spectrum as a whole to minimize the total current harmonic distortion.

Experimental measurements of the THD_i of the motor currents for the system at rated conditions, with 380 V ($M \approx 1.05$) and 90 Hz fundamental output voltage and mechanical shaft power of 11.5 kW at 1800 rpm, operating with SOP, SHE, SVM, and mIPD modulations for a variety of switching frequencies are presented in Fig. 11. The measurements were performed with a power analyzer Yokogawa WT1800 and a oscilloscope LeCroy 610Zi with, respectively, ADP305 and CP031 voltage

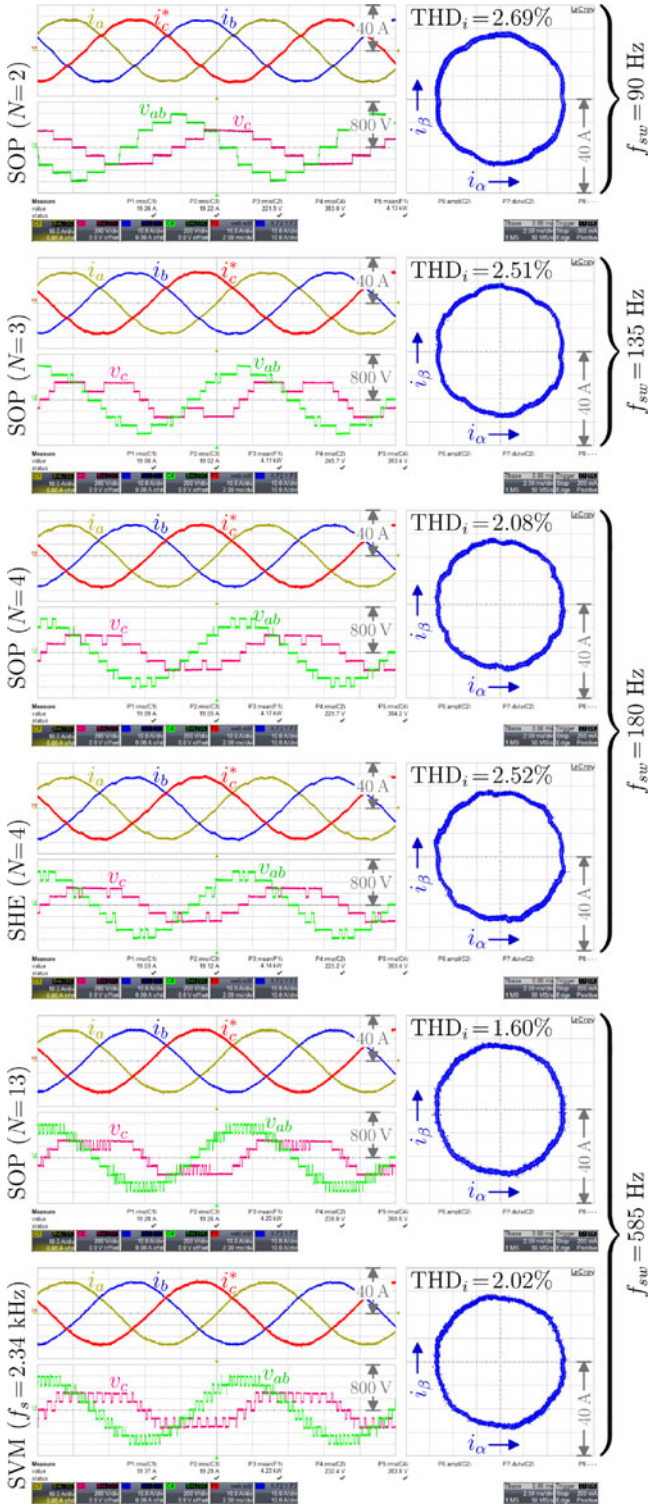

Fig. 11. Experimental results voltage and current waveforms with SHE, SOP, and SVM modulation for a variety of switching frequencies with $M = 1.05$.

and current probes. Fig. 11 shows a phase voltage, a line-to-line voltage and the motor current waveforms as well as the motor currents trajectory in the $\alpha\beta$ plane for some of the experiments.

The motor current average THD (THD_i) measurements include up to the 50th harmonic (4.5 kHz). As expected the SOP modulation presented the best results, with low levels of load

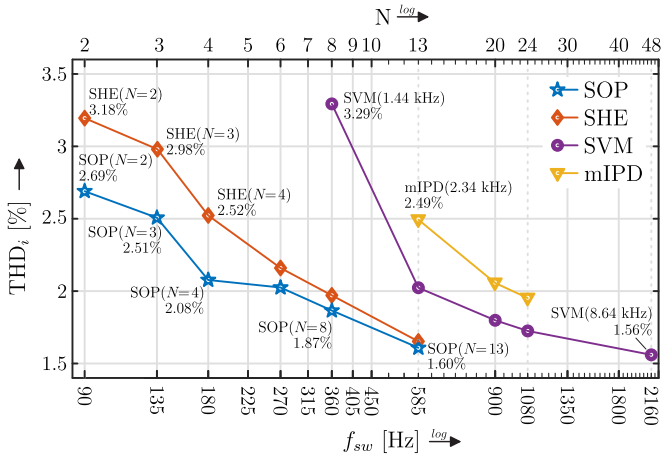

Fig. 12. Experimental results comparison between SHE, SOP, SVM, and mIPD modulation for a variety of switching frequencies with $M = 1.05$.

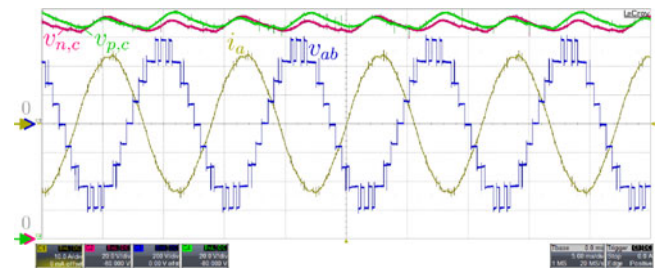

Fig. 13. Experimental results: two dc-link voltages $v_{n,c}$ and $v_{p,c}$, line voltage v_{ab}, and phase current i_a waveforms with the proposed SOP operating with $M = 1.05$, $f_1 = 90$ Hz, $N = 4$, and $f_{\text{sw}} = 180$ Hz.

current harmonic distortion even for very low switching frequency, i.e., $\text{THD}_i = 2.69\%$ for $N = 2$, condition in which each power semiconductor device operates at the same frequency as the fundamental, with a device switching frequency of $f_{\text{sw}} = 90$ Hz for a fundamental frequency of 90 Hz. The SVM with switching frequency four times higher ($f_{\text{sw}} = 360$ Hz is equivalent to a sampling frequency of 1.44 kHz for the HNPC) achieves only $\text{THD}_i = 3.29\%$. With the same device switching frequency ($f_{\text{sw}} = 360$ Hz) the SOP modulation presents a decrease in the current distortion of 43% with respect to SVM, where $\text{THD}_i = 1.87\%$. The results are summarized in Fig. 12.

Fig. 13 shows a line-to-line voltage and the a motor current waveforms as well as the positive and negative dc-link voltages that are actively balanced by choosing redundant states in the second modulation step. Experimental results for the SOP modulation are presented in Fig. 14 for a variety of operating points of Fig. 6 using a V/f relationship given by

$$M = \frac{f_1}{f_{1R}} M_R \tag{16}$$

were R index stands for rated value and $M_R = 1.05$ and $f_{1R} = 90$ Hz. Results for different modulation indexes, fundamental frequencies, and switching transitions per cycle are observed as well as the current vector trajectories for each operating condition.

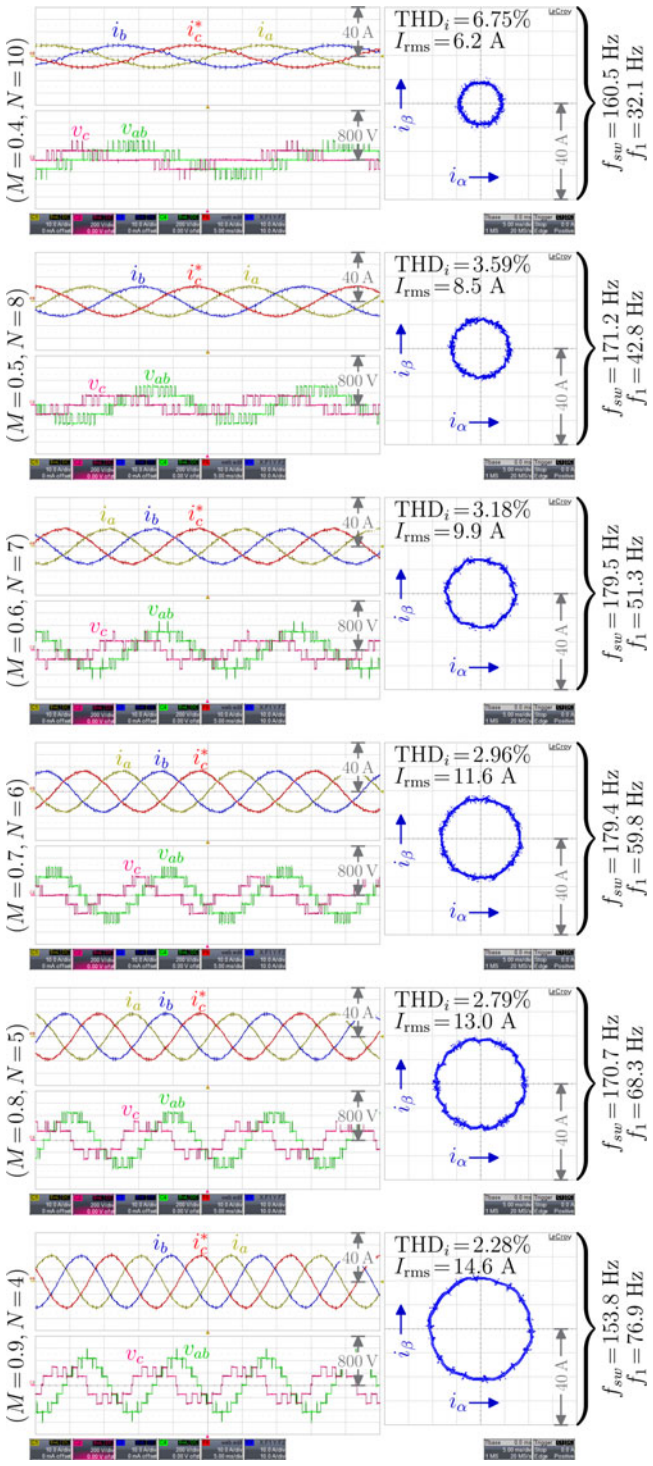

Fig. 14. Experimental results showing voltage and current waveforms with the proposed SOP for a variety of modulation indexes and fundamental frequencies with constant V/f.

IV. Conclusion

This work proposed a way to overcome the complexities of optimizing the modulation of multilevel inverters. The presented formulation does not use the switching patterns concept and, thus, is a generalized formulation for the problem. It does so by including the transition directions decision into the optimization problem as an expansion of the search space of the optimization variables. A comparison of this technique with the conventional one validated the formulation. The effectiveness of the proposed technique was experimentally tested in a 3-phase HNPC feeding a PMSM. These experiments were performed in a wide range of commutations per cycle range that shows that the proposed SOP formulation can deal with generic multilevel waveforms, both with low or high number of switching patterns. The results with very few commutations per cycle show that the SOP overcomes the limitations of nonoptimal modulations with a $\text{THD}_i = 2.69\%$ even when the IGBTs switch at the fundamental frequency.

Appendix

The presented formulation used phase voltage waveforms. Nonetheless, the line currents are ultimately generated by the line-to-line voltages. However, the equivalent line-to-line voltage waveform composed by L levels phase waveforms with N commutation per quarter-cycle has $(2L-1)$ levels and $2N$ commutations per quarter-cycle results in a much larger optimization problem without additional degree of freedom. The following proves that optimizing the phase voltage waveform considering only the nontriplen harmonic components is equivalent to optimizing the line-to-line voltages.

The line-to-line voltage is defined from (1) as

$$l^{\text{ab}}(\theta) = l^{a}(\theta) - l^{b}(\theta) = \sum_{k=1}^{N} \left[\xi_k(\theta) - \xi_k(\theta - 2\pi/3)\right] \quad (17)$$

which has the harmonic contents given by

$$\hat{l}_h^{\text{ab}}(\boldsymbol{\gamma}) = \frac{1}{\pi h}\sum_{k=1}^{N}\left[\sin\left(h\gamma_k - \frac{h\pi}{6}\right) + \sin\left(h\gamma_k + \frac{h\pi}{6}\right)\right]$$
$$= \frac{\sqrt{3}}{\pi h}\sum_{k=1}^{N}\sin(h\gamma_k)g(h) \quad (18)$$

with

$$g(h) = \frac{2}{\sqrt{3}}\cos\left(h\frac{\pi}{6}\right). \quad (19)$$

Apart from the term $g(h)$, (18) has the same form as (10). In fact $g(h)$ is the term that models the line-to-line voltage spectrum triplen harmonics cancellations due to the $2\pi/3$ phase-shift between two phase voltages. Since

$$g(h = \{1,3,5,7,9,11,13,15,17,\ldots\})$$
$$= \{+1,0,-1,-1,0,+1,+1,0,-1\ldots\} \quad (20)$$

it follows that:

$$\left|\hat{l}^{\text{ab}}(\boldsymbol{\gamma})\right| = \begin{cases} \sqrt{3}\left|\hat{l}(\boldsymbol{\gamma})\right| & \text{if } h \text{ is odd and nontriplen} \\ 0 & \text{otherwise} \end{cases} \quad (21)$$

and as the phase angles of the harmonic components are not relevant for the optimization process, the line-to-line waveform is optimized when the spectrum of the phase components accounting for only the nontriplen harmonics as done in (6).

REFERENCES

[1] F. Turnbull, "Selected harmonic reduction in static dc-ac inverters," *IEEE Trans. Commun.*, vol. 83, no. 73, pp. 374–378, Jul. 1964.

[2] G. S. Buja and G. B. Indri, "Optimal pulsewidth modulation for feeding ac motors," *IEEE Trans. Ind. Appl.*, vol. IA-13, no. 1, pp. 38–44, Jan. 1977.

[3] R. Rathore, H. Holtz, and T. Boller, "Generalized optimal pulsewidth modulation of multilevel inverters for low-switching-frequency control of medium-voltage high-power industrial ac drives," *IEEE Trans. Ind. Electron.*, vol. 60, no. 10, pp. 4215–4224, Oct. 2013.

[4] N. Oikonomou and J. Holtz, "Closed-loop control of medium-voltage drives operated with synchronous optimal pulsewidth modulation," *IEEE Trans. Ind. Appl.*, vol. 44, no. 1, pp. 115–123, Jan. 2008.

[5] Y. Liu, Z. Du, A. Huang, and S. Bhattacharya, "An optimal combination modulation strategy for a seven-level cascade multilevel converter based statcom," in *Proc. 2006 41st IAS Annu. Meet. IEEE Ind. Appl. Conf.*, Oct. 2006, vol. 4, pp. 1732–1737.

[6] J. Holtz and X. Qi, "Optimal control of medium-voltage drives—An overview," *IEEE Trans. Ind. Electron.*, vol. 60, no. 12, pp. 5472–5481, Dec. 2013.

[7] J. Holtz, G. da Cunha, N. Petry, and P. Torri, "Control of large salient-pole synchronous machines using synchronous optimal pulsewidth modulation," *IEEE Trans. Ind. Electron.*, vol. 62, no. 6, pp. 3372–3379, Jun. 2015.

[8] A. Ghias, J. Pou, V. Agelidis, and M. Ciobotaru, "Optimal switching transition-based voltage balancing method for flying capacitor multilevel converters," *IEEE Trans. Power Electron.*, vol. 30, no. 4, pp. 1804–1817, Apr. 2015.

[9] A. Edpuganti and A. Rathore, "New optimal pulsewidth modulation for single dc-link dual-inverter fed open-end stator winding induction motor drive," *IEEE Trans. Power Electron.*, vol. 30, no. 8, pp. 4386–4393, Aug. 2015.

[10] A. Edpuganti and A. Rathore, "Fundamental switching frequency optimal pulsewidth modulation of medium-voltage nine-level inverter," *IEEE Trans. Ind. Electron.*, vol. 62, no. 7, pp. 4096–4104, Jul. 2015.

[11] A. Edpuganti and A. Rathore, "Optimal low-switching frequency pulsewidth modulation of medium voltage seven-level cascade-5/3h inverter," *IEEE Trans. Power Electron.*, vol. 30, no. 1, pp. 496–503, Jan. 2015.

[12] T. Boller, J. Holtz, and A. Rathore, "Neutral-point potential balancing using synchronous optimal pulsewidth modulation of multilevel inverters in medium-voltage high-power ac drives," *IEEE Trans. Ind. Appl.*, vol. 50, no. 1, pp. 549–557, Jan. 2014.

[13] A. Edpuganti and A. Rathore, "Fundamental switching frequency optimal pulsewidth modulation of medium-voltage cascaded seven-level inverter," *IEEE Trans. Ind. Appl.*, vol. 51, no. 4, pp. 3485–3492, Jul. 2015.

[14] J. Lago and M. Lobo Heldwein, "Multilevel synchronous optimal pulsewidth modulation generalized formulation," in *Proc. 2014 IEEE 15th Workshop Control Model. Power Electron.*, Jun. 2014, pp. 1–7.

[15] H. S. Patel, "Thyristor inverter harmonic elimination using optimization techniques," Ph.D. dissertation, Dept. Electr. Eng., Univ. Missouri, Columbia, MO, USA, 1971.

[16] H. S. Patel and R. Hoft, "Generalized techniques of harmonic elimination and voltage control in thyristor inverters: Part i–harmonic elimination," *IEEE Trans. Ind. Appl.*, vol. IA-9, no. 3, pp. 310–317, May 1973.

[17] H. S. Patel and R. Hoft, "Generalized techniques of harmonic elimination and voltage control in thyristor inverters: Part ii—Voltage control techniques," *IEEE Trans. Ind. Appl.*, vol. IA-10, no. 5, pp. 666–673, Sep. 1974.

[18] F. C. Zach, R. Martinez, S. Keplinger, and A. Seiser, "Dynamically optimal switching patterns for PWM inverter drives (for minimization of the torque and speed ripples)," *IEEE Trans. Ind. Appl.*, vol. IA-21, no. 4, pp. 975–986, Jul. 1985.

[19] J. Wells, B. Nee, P. Chapman, and P. Krein, "Optimal harmonic elimination control," in *Proc. 2004 IEEE 35th Annu. Power Electron. Spec. Conf.*, 2004, vol. 6, pp. 4214–4219.

[20] J. Hobraiche, J. Vilain, and C. Plasse, "Offline optimized pulse pattern with a view to reducing dc-link capacitor application to a starter generator," in *Proc. 2004 IEEE 35th Annu. Power Electron. Spec. Conf.*, 2004, vol. 5, pp. 3336–3341.

[21] C. Namuduri and P. Sen, "Optimal pulsewidth modulation for current source inverters," *IEEE Trans. Ind. Appl.*, vol. IA-22, no. 6, pp. 1052–1072, Nov. 1986.

[22] A. Rathore, J. Holtz, and T. Boller, "Synchronous optimal pulsewidth modulation for low-switching-frequency control of medium-voltage multilevel inverters," *IEEE Trans. Ind. Electron.*, vol. 57, no. 7, pp. 2374–2381, Jun. 2010.

[23] J. Chiasson, L. Tolbert, K. McKenzie, and Z. Du, "Eliminating harmonics in a multilevel converter using resultant theory," in *Proc. 2002 IEEE 33rd Annu. Power Electron. Spec. Conf.*, 2002, vol. 2, pp. 503–508.

[24] J. N. Chiasson, L. M. Tolbert, K. J. McKenzie, and Z. Du, "Control of a multilevel converter using resultant theory," *IEEE Trans. Control Syst. Technnol.*, vol. 11, no. 3, pp. 345–354, May 2003.

[25] J. Meili, S. Ponnaluri, L. Serpa, P. Steimer, and J. Kolar, "Optimized pulse patterns for the 5-level ANPC converter for high speed high power applications," in *Proc. 2006 32nd Conf. Ind. Electron.*, Nov. 2006, pp. 2587–2592.

[26] Y. Liu, H. Hong, and A. Huang, "Real-time calculation of switching angles minimizing THD for multilevel inverters with step modulation," *IEEE Trans. Ind. Electron.*, vol. 56, no. 2, pp. 285–293, Mar. 2009.

[27] Z. Du, L. Tolbert, and J. Chiasson, "Active harmonic elimination in multilevel converters using FPGA control," in *Proc. 2004 IEEE Workshop Comput. Power Electron.*, 2004, pp. 127–132.

[28] J. Wells, P. Chapman, and P. Krein, "Generalization of selective harmonic control/elimination," in *Proc. 2005. IEEE 36th Power Electron. Spec. Conf.*, 2005, pp. 1358–1363.

[29] J. Wells, B. Nee, P. Chapman, and P. Krein, "Selective harmonic control: A general problem formulation and selected solutions," *IEEE Trans. Power Electron.*, vol. 20, no. 6, pp. 1337–1345, Nov. 2005.

[30] J. Holtz and B. Beyer, "Optimal synchronous pulsewidth modulation with a trajectory-tracking scheme for high-dynamic performance," *IEEE Trans. Ind. Appl.*, vol. 29, no. 6, pp. 1098–1105, Nov./Dec. 1993.

[31] Q. Song, W. Liu, and Z. Yuan, "Multilevel optimal modulation and dynamic control strategies for statcoms using cascaded multilevel inverters," *IEEE Tran Pow. Del.*, vol. 22, no. 3, pp. 1937–1946, Jul. 2007.

[32] P. Kujan, M. Hromcik, and M. Sebek, "Complete fast analytical solution of the optimal odd single-phase multilevel problem," *IEEE Trans. Ind. Electron.*, vol. 57, no. 7, pp. 2382–2397, Jul. 2010.

[33] J. Lago, G. Sousa, and M. Heldwein, "Digital control/modulation platform for a modular multilevel converter system," in *Proc. 2013 Power Electron. Brazilian Conf.*, Oct. 2013, pp. 271–277.

[34] G. Konstantinou, M. Ciobotaru, and V. Agelidis, "Selective harmonic elimination pulse-width modulation of modular multilevel converters," *IEEE Trans. Power Electron.*, vol. 6, no. 1, pp. 96–107, Jan. 2013.

[35] H. Mohammadi and A. Akhavan, "A new adaptive selective harmonic elimination method for cascaded multilevel inverters using evolutionary methods," in *Proc. 2014 IEEE 23rd Int. Symp. Ind. Electron.*, Jun. 2014, pp. 1484–1489.

[36] M. Dahidah, G. Konstantinou, and V. Agelidis, "A review of multilevel selective harmonic elimination PWM: Formulations, solving algorithms, implementation and applications," *IEEE Trans. Power Electron.*, vol. 30, no. 8, pp. 4091–4106, Aug. 2015.

[37] J. Napoles *et al.*, "Selective harmonic mitigation technique for cascaded h-bridge converters with nonequal dc link voltages," *IEEE Trans. Ind. Electron.*, vol. 60, no. 5, pp. 1963–1971, May 2013.

[38] C. Buccella, C. Cecati, M. Cimoroni, and K. Razi, "Analytical method for pattern generation in five-level cascaded h-bridge inverter using selective harmonic elimination," *IEEE Trans. Ind. Electron.*, vol. 61, no. 11, pp. 5811–5819, Nov. 2014.

[39] S. Pulikanti and V. Agelidis, "Five-level active NPC converter topology: SHE-PWM control and operation principles," in *Proc. 2007 Power Eng. Conf. Australasian Univ.*, Dec. 2007, pp. 1–5.

[40] W. Fei, X. Ruan, and B. Wu, "A generalized formulation of quarter-wave symmetry SHE-PWM problems for multilevel inverters," *IEEE Trans. Power Electron.*, vol. 24, no. 7, pp. 1758–1766, Jul. 2009.

[41] V. Agelidis, A. Balouktsis, and C. Cossar, "On attaining the multiple solutions of selective harmonic elimination PWM three-level waveforms through function minimization," *IEEE Trans. Ind. Electron.*, vol. 55, no. 3, pp. 996–1004, Mar. 2008.

[42] W. Fei, X. Du, and B. Wu, "A generalized half-wave symmetry SHE-PWM formulation for multilevel voltage inverters," *IEEE Trans. Ind. Electron.*, vol. 57, no. 9, pp. 3030–3038, Sep. 2010.

[43] Z. Cheng and B. Wu, "A novel switching sequence design for five-level NPC/h-bridge inverters with improved output voltage spectrum and minimized device switching frequency," in *Proc. 2006 37th IEEE Power Electron. Spec. Conf.*, Jun. 2006, pp. 1–6.

[44] Y. Pei *et al.*, "Investigation on the control strategy of high power NPC/h-bridge inverter," in *Proc. Int. Conf. Electr. Mach. Syst.*, Oct. 2013, pp. 1670–1673.

Jackson Lago received the B.S. degrees in electrical engineering from the University Center of Jaraguá do Sul (UNERJ), Jaraguá do Sul, Brazil, in 2009, and the M.S. and Ph.D degrees in electrical engineering from the Federal University of Santa Catarina (UFSC), Florianópolis, Brazil, in 2011 and 2015, respectively.

From 2015 to 2016 he was a researcher at the Power Electronics Institute (INEP) of the Federal University of Santa Catarina (UFSC). He is currently an Adjunct Professor with the Electrotechnical Department at the Federal Institute of Education, Science and Technology of Santa Catarina (IFSC). His research interests include power electronics and electrical machines drives.

Marcelo Lobo Heldwein (S'99-M'08-SM'13) received the B.S. and M.S. degrees in electrical engineering from the Federal University of Santa Catarina (UFSC), Florianópolis, Brazil, in 1997 and 1999, respectively, and the Ph.D. degree from the Swiss Federal Institute of Technology (ETH Zurich), Zurich, Switzerland, in 2007.

He is currently an Adjunct Professor with the Electronics and Electrical Engineering Department at the UFSC. From 1999 to 2003, he worked with industry, including research at the Power Electronics Institute, Brazil and Emerson Network Power, Brazil and Sweden. He was a Postdoctoral Fellow at the ETH Zurich and at the UFSC from 2007 to 2009.

Dr. Heldwein is a member of the Brazilian Power Electronic Society (SOBRAEP). His research interests include power electronics, power distribution, and electromagnetic compatibility.